Analyst

Rapid Capture of Biomolecules from Blood via Stimuli-Responsive Elastomeric Particles for Acoustofluidic Separation

Journal:	*Analyst*
Manuscript ID	AN-ART-06-2020-001164.R1
Article Type:	Paper
Date Submitted by the Author:	29-Sep-2020
Complete List of Authors:	Li, Linying; NSF Research Triangle Materials Research Science and Engineering Center; Duke University, Department of Biomedical Engineering Shields, C. Wyatt; University of Colorado at Boulder, Chemical and Biological Engineering; NSF Research Triangle Materials Research Science and Engineering Center; Duke University Department of Biomedical Engineering, Huang, Jin; Duke University, Department of Biomedical Engineering Zhang, Yiqun; Duke University, Department of Biomedical Engineering Ohiri, Korine; NSF Research Triangle Materials Research Science and Engineering Center; Duke University, Department of Mechanical Engineering and Materials Science Yellen, Benjamin; Duke University, Department of Mechanical Engineering and Materials Science; Duke University Department of Biomedical Engineering, Chilkoti, Ashutosh; NSF Research Triangle Materials Research Science and Engineering Center; Duke University Department of Biomedical Engineering, ; Duke University, Department of Mechanical Engineering and Materials Science Lopez, Gabriel; University of New Mexico, Department of Chemical and Nuclear Engineering; NSF Research Triangle Materials Research Science and Engineering Center; Duke University Department of Biomedical Engineering, ; Duke University, Department of Mechanical Engineering and Materials Science

Rapid Capture of Biomolecules from Blood via Stimuli-Responsive Elastomeric Particles for Acoustofluidic Separation

Linying Li,[1,2] C. Wyatt Shields IV,[1,2,3*] Jin Huang,[2] Yiqun Zhang,[2] Korine A. Ohiri,[1,4] Benjamin B. Yellen,[1,4] Ashutosh Chilkoti[1,2,4] and Gabriel P. López[1,2,4,5*]

1. NSF Research Triangle Materials Research Science and Engineering Center, Durham, NC 27708, USA
2. Department of Biomedical Engineering, Duke University, Durham, NC 27708, USA
3. Department of Chemical and Biological Engineering, University of Colorado Boulder, Boulder, CO 80303, USA
4. Department of Mechanical Engineering and Materials Science, Duke University, Durham, NC 27708, USA
5. Center for Biomedical Engineering, Department of Chemical and Biological Engineering, University of New Mexico, Albuquerque, NM 87131, USA

***Corresponding authors:** gplopez@unm.edu and charles.shields@colorado.edu

Submitted to: *The Analyst*

Keywords: Acoustofluidics, elastomeric particles, elastin-like polypeptides (ELPs), biosensing, biomarkers, co-aggregation, bioseparation

Abstract

The detection of biomarkers in blood often requires extensive and time-consuming sample preparation to remove blood cells and concentrate the biomarker(s) of interest. We demonstrate proof-of-concept for a chip-based, acoustofluidic method that enables the rapid capture and isolation of a model protein biomarker (i.e., streptavidin) from blood for off-chip quantification. Our approach makes use of two key components – namely, soluble, thermally responsive polypeptides fused to ligands for the homogeneous capture of biomarkers from whole blood and silicone microparticles functionalized with similar, tethered, thermally responsive polypeptides. When the two components are mixed together and subjected to a mild thermal trigger, the thermally responsive moieties undergo a phase transition, causing the untethered (soluble) polypeptides to co-aggregate with the particle-bound polypeptides. The mixture is then diluted with warm buffer and injected into a microfluidic channel supporting a bulk acoustic standing wave. The biomarker-bearing particles migrate to the pressure antinodes, whereas blood cells migrate to the pressure node, leading to rapid separation with efficiencies exceeding 90% in a single pass. The biomarker-bearing particles can then be analyzed via flow cytometry, with a limit of detection of 0.75 nM for streptavidin spiked in blood plasma. Finally, by cooling the solution below the solubility temperature of the polypeptides, greater than 75% of the streptavidin is released from the microparticles, offering a unique approach that for downstream analysis (e.g., sequencing or structural analysis). Overall, this methodology has promise for the detection, enrichment and analysis of some biomarkers from blood and other complex biological samples.

Introduction

The separation, detection and quantification of biomarkers from blood is increasingly necessary for disease diagnosis, prognosis and screening patient responses to drugs and therapeutic interventions.[1–4] However, the analysis of biomarkers presents several challenges, such as nonspecific interactions between cellular or subcellular entities[5,6] and low concentrations of clinically relevant biomarkers present during early disease states.[7,8] Traditional technologies for diagnosis include enzyme-linked immunosorbent assay (ELISA), nucleic acid hybridization, amplification and sequencing, microbial culture and mass spectrometry, most of which require significant sample preparation prior to analysis.[9–11] While centrifugation is commonly performed as a first step to remove cells, this method is time-consuming, requires bulky instrumentation, necessitates relatively large sample volumes and frequently results in a significant loss of biomarkers.[12,13] In addition, more involved methods (e.g., chromatography or electrophoresis) are sometimes required to further isolate and purify biomarkers.[14–16] There is thus a critical need for a simple strategy to rapidly separate and enrich biomarkers from blood prior to downstream quantification and analysis.

Acoustofluidics offers a convenient approach to remove blood cells and purify biomarkers prior to their quantification.[17–26] Our group has demonstrated that negative acoustic contrast particles made from silicone elastomers can be continuously separated from positive acoustic contrast objects (e.g., cells or polystyrene beads) in an acoustic standing wave.[22,25–27] This separation process is based on inducing acoustic radiation forces on particles and cells towards different stable positions along the standing wave. These positions depend on the acoustic contrast factor:

$$\varphi(\beta,\rho) = \frac{5\rho_p - 2\rho_f}{2\rho_p + \rho_f} - \frac{\beta_p}{\beta_f},$$

where variables ρ and β represent density and compressibility, respectively, and the subscripts p and f represent the suspended object (e.g., particle or cell) and the fluid medium, respectively.[28–33] Objects exhibiting positive acoustic contrast move towards the pressure node, which is located along the centerline of a microfluidic channel when the channel width is equal (or nearly equal) to one half of the acoustic wavelength.[34] Alternatively, objects exhibiting negative acoustic contrast, such as elastomeric particles, migrate to the pressure antinodes, which are located near the walls of the microfluidic channel. By engineering a trifurcating outlet in such a microfluidic system, objects flowing along the walls can exit the peripheral (herein referred to as “collection”) outlets, and objects flowing near the centerline can exit the central (“waste”) outlet, thus enabling continuous and discriminant separation of elastomeric particles from cells.[22]

Previously, our lab has shown that polydisperse, negative acoustic contrast particles made from polydimethylsiloxane (PDMS) with physically adsorbed surface ligands can enable the detection of biomarkers in diluted blood.[22] To build upon this work, we use a class of acoustically programmable particles comprised of silicone elastomers that can be synthesized in bulk and are nearly monodisperse (i.e., whereby the coefficient of variance (C.V.) in size is less than 15%).[35] We show that the surfaces of these particles can be covalently functionalized with thermally responsive polypeptides to rapidly capture biomarkers through thermally triggered co-aggregation. Captured biomarkers can then be acoustically separated from blood and quantified via flow cytometry or released for recovery, enrichment and further analysis.

To achieve the thermally triggered co-aggregation functionality, we modified the silicone particles with genetically engineered, thermally responsive, elastin-like polypeptides (ELPs). ELPs consist of a pentapeptide repeating motif (Val-Pro-Gly-Xaa-Gly, where Xaa represents any amino acid except Pro) and can be genetically modified to incorporate short peptide sequences to capture bioactive molecules.[36–40] Instead of immobilizing the capture ligands on a surface, as in ELISA, we conjugated capture ligands to untethered ELPs to capture model biomarkers in solution. The mobility of soluble ELP-ligand fusions should allow for homogenous binding kinetics,[41] which may allow a reduction of the required incubation time for immunoassays. Additionally, by working at high concentrations of the ELP-ligand conjugate in biological fluids, the capture process can be driven nearly to completion. As a model testbed, we used biotin as the capture ligand and streptavidin (SA) as the model biomarker in this study due to their strong binding interaction (dissociation constant $K_d = 10^{-15}$ M)[42,43] and low cost.

Figure 1a,b depicts the capture of biomarkers in blood via a soluble ELP-ligand conjugate. To capture ELP-ligand/biomarker complexes on the surfaces of the particles, we exploited the lower critical solution temperature (LCST) phase transition behavior of ELPs in water, in which ELPs at a given concentration phase separate to form protein-rich coacervates above the cloud point transition temperature (T_t).[44,45] In previous studies, it was shown that ELP-modified glass substrates can reversibly capture and release untethered ELP fusion proteins (thioredoxin-ELP) in response to changes in temperature.[46,47] In a similar approach, Stayton *et al.* used thermally responsive poly(N-isopropylacrylamide) (pNIPAAm)-modified substrates (i.e., PDMS, nylon) to capture and enrich pNIPAAm-protein conjugates via co-aggregation above the LCST.[48,49] Building on these concepts, we hypothesized that ELP-modified silicone particles can co-aggregate with an ELP- functionalized ligand (hereafter referred to as ELP-ligand) in solution to facilitate the rapid capture and sequestration of biomarkers after a small increase in temperature (e.g., 15°C; Figure 1c,d). After the capture of biomarkers, the silicone particles can be separated from blood cells using an acoustofluidic device (Figure 1e). The particles can then be analyzed by flow cytometry to quantify the immobilized biomarkers, or alternatively, collected in a small volume of buffer at a reduced temperature to facilitate the release of biomarkers (Figure 1f).

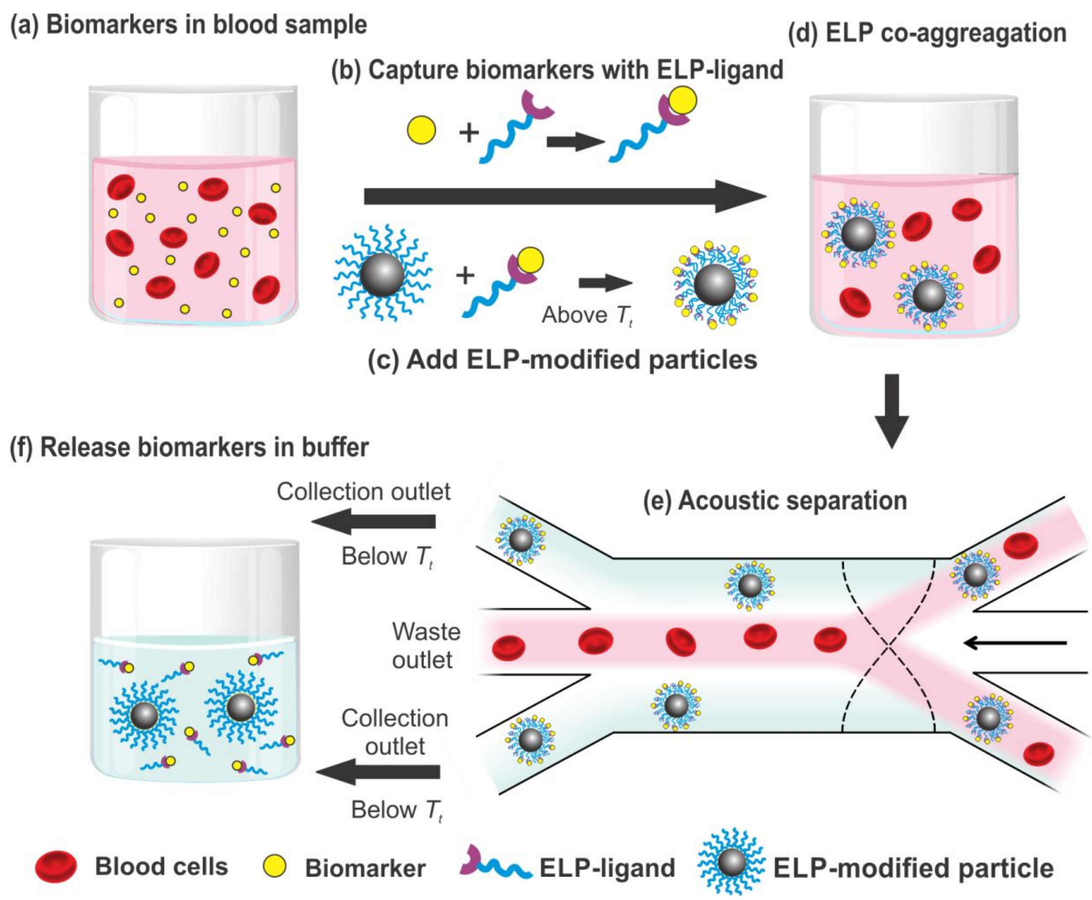

Figure 1. Schematic illustration of the process for capturing and acoustically separating biomarkers from blood. (a-b) Untethered ELP-ligands capture biomarkers in blood. Pink color of solution is meant to reflect the color of red blood cells, a few of which are depicted schematically. (c-d) Above the cloud point transition temperature (T_t) of the ELPs, ELP-coated silicone particles are added to immobilize ELP-ligand/biomarker complexes to the surfaces of the particles via co-aggregation. (e) After dilution of the mixture with warm buffer, an acoustofluidic device is used to separate captured biomarkers from blood cells. (f) Surface-immobilized biomarkers can then be analyzed by flow cytometry or released from the surfaces of the particles below the T_t. Figure is not to scale.

Experimental

Synthesis of negative acoustic contrast silicone particles

The silicone particles used in this study were synthesized using methods described previously.[35] Briefly, silicone particles were made from a 24:1 monomer ratio of vinyl methyldimethoxysilane (VMDMOS, 97% purity; Sigma-Aldrich, Co.) to tetramethyl orthosilicate (TMOS; 98% purity, Sigma-Aldrich). Our previous work indicates that these particles possess an acoustic contrast factor, φ, of –0.37±0.07.[35] Immediately following their synthesis, the particles were stabilized in 0.5 wt.% F-108 surfactant in deionized water (Pluronic; Sigma-Aldrich). The silicone particles had an average diameter of 1.5±0.2 µm and a concentration of ~10^9 particles/mL, as measured by the Coulter sizing and counting principle (qNano; IZON Science, Ltd.).

Elastin-like polypeptide (ELP) constructs

The ELPs investigated in this study consisted of repeats of the Val-Pro-Gly-Val-Gly pentapeptide, with a Ser-Lys-Gly-Pro-Gly leader sequence. In some constructs, 8 tandem repeats of (Gly-Gly-Cys) were included as a trailer sequence, facilitating the conjugation of these ELPs to the vinyl groups on silicone particles via a thiol-ene reaction,[50,51] as described below. The amino acid sequences of the ELP constructs were SKGPG$(VGVPG)_{40}(GGC)_8$WP (termed ELP-Cys herein) and SKGPG$(VGVPG)_{40}$Y (termed ELP), each of which was expressed from plasmids available from a previous study.[52]

To build the gene encoding for the GFP-ELP-Cys fusion protein, the GFP gene was retrieved from a previously available plasmid, GFP-ELP,[53] by PCR and followed by double digestion of PCR products with BseRI and NdeI restriction enzymes (New England BioLabs, Inc.). The pET 24a plasmids harboring 40 repeating pentapeptides (Val-Pro-Gly-Val-Gly) and a trailer sequence of (Gly-Gly-Cys)$_8$ were also double digested with the same restriction enzymes (i.e., BseRI and NdeI), and then enzymatically dephosphorylated using calf intestinal alkaline phosphatase (New England BioLabs). The linearized vectors encoding for ELPs were separated from other DNA fragments by gel electrophoresis with low temperature melting agarose (AquaPor LM; National Diagnostics, Inc.), and were purified using an extraction kit (QIAquick® gel; Qiagen, Inc.). The purified ELP vectors were ligated with the GFP gene to create a plasmid-harboring gene for the GFP-ELP-Cys fusion proteins. Correct assembly of the gene for the GFP-ELP-Cys fusion protein was confirmed by DNA sequencing. The final amino acid sequence of the construct containing GFP was determined to be GFP-(VGVPG)$_{40}$ (GGC)$_8$WP (referred to as GFP-ELP-Cys herein).

Expression and purification of ELPs

All of the ELPs and the GFP-ELP-Cys fusion proteins were expressed in BL21(DE3) *E. coli* and purified by inverse transition cycling, as described previously.[54] These purified ELPs and GFP-ELP-Cys were characterized by sodium dodecyl sulfate polyacrylamide gel electrophoresis (SDS-PAGE; BioRad, Inc.). An image of the resulting gel is shown in Figure S1 in the Supplementary Information. After purification, the optical densities at 350 nm (OD$_{350}$) of the different types of ELPs in PBS buffer were measured as a function of temperature to characterize their aqueous phase behaviors (see Figure S2 in the Supplementary Information for more details). Samples were heated at 1°C/min in a UV-visible spectrophotometer equipped with a multi-cell thermoelectric temperature controller (Cary 300; Varian, Inc.).

Labeling ELPs with biotin for protein capture

The ELP construct, SKGPG(VGVPG)$_{40}$Y, (herein referred to as ELP-40) has two primary amines, one at the N-terminus and one in the lysine residue in the leader sequence, which allowed conjugation reactions using N-hydroxysuccinimide (NHS) ester chemistry.[55] A 150 μM solution of this ELP was reacted with a 20-fold molar excess of NHS-activated biotin (sulfo-NHS-biotin; Thermo Fisher Scientific, Inc.) dissolved in water for 2 h at room temperature. The excess biotin derivatives were removed using spin desalting columns (Zeba™; Thermo Fisher). To determine the efficiency of the biotinylation reaction, a 4'-hydroxyazobenzene-2-carboxylic acid (HABA) assay was used according to the instructions provided by the manufacturer (Thermo Fisher). The labeling efficiency was found to be between 0.9-1.5 biotins/ELP. The biotinylated ELP constructs are herein referred to as biotin-ELP.

Conjugation of ELPs to silicone particles

We used GFP-ELP-Cys fusions and ELPs with a $(VPGVG)_{40}$ sequence and a cysteine-rich domain $(GGC)_8$ (herein referred to as ELP-Cys) to conjugate ELPs to the surfaces of the silicone particles. The thiol groups present in the cysteine residues were conjugated to the vinyl groups on silicone particles via a thiol-ene reaction facilitated by UV irradiation.[50,51] The silicone particles (100 μL at ~10^9 particles/mL) were directly added to the ELP solutions (900 μL) to obtain a final concentration of 150 μM ELP. The reaction was carried out at room temperature under UV irradiation (wavelength of 365 nm and a power intensity of 100 μW/cm^2, UVGL-15; Entela, Inc.) for 2 h with constant stirring at 300 rpm. As a control, the same process was carried out without UV irradiation to assess the degree of nonspecific physical adsorption of ELPs to the surfaces of the particles. Prior to use for different assays, particles were washed (i.e., centrifuged at 4000xG for 2.5 min and the pellet was suspended in fresh PBS at ~10^8 particles/mL) to remove excess ELPs.

Quantification of GFP-ELP-Cys peptides bound to silicone particles

We used flow cytometry (Accuri C6; BD Biosciences) to evaluate the average number of GFP-ELP-Cys molecules associated with each particle after the UV-induced reaction or physical adsorption.[56] The autofluorescence signal of bare silicone particles was measured as a baseline. The flow cytometry data were acquired from at least five independent measurements and were gated on forward and side scatter parameters to exclude debris and doublets. A calibration test was conducted using a set of calibration beads (8-peak SPHERO^{TM} Rainbow Calibration particles; Spherotech, Inc.) to convert the raw data (i.e., channel counts) into molecules equivalent of fluorescence (MEFL) of fluorophores per particle. In these experiments, the molecules of GFP-ELP-Cys per particle are equal to the MEFL, as one GFP molecule was present on each ELP. A similar quantification approach has been used previously.[35]

The GFP-ELP-Cys-modified particles were visualized using an upright confocal, scanning laser microscope (Zeiss LSM 780; Carl Zeiss AG) with a dry plan-apochromat objective (20x, 0.8 numerical aperture (NA) and oil plan-apochromat 63x, oil-immersion objective, 1.4 NA; Zeiss). The GFPs were excited by light with a wavelength of 488 nm. Images were processed offline with imaging software (Imaris 7.5; Bitplane, Inc.).

Capture of protein biomarkers via the co-aggregation of ELPs

To demonstrate proof-of-concept of biomarker isolation, we used fluorescent SA conjugated to Alexa Fluor 488 (Thermo Fisher) as a model biomarker that can be captured by biotin-ELP. To perform the capture and co-aggregation assay, we first spiked 100 μL of PBS with 5 μM fluorescent SA, followed by 200 μM biotin-ELP. After 10 min of incubation, the silicone particles with UV-reacted ELPs (20 μL at ~10^8 particles/mL) were added to the mixture and incubated at 40°C for 5 min to trigger the ELP co-aggregation. Bare particles and particles with physically adsorbed ELPs were used as controls. The fluorescence intensities of particles in all experimental conditions were measured using flow cytometry to estimate the number of SA per particle. To perform these experiments, we heated the sheath fluid in the flow cytometer to above 40°C to ensure that the ELPs remained stably co-aggregated throughout the measurement. In addition, to quantify the non-specific adsorption of SA to the surfaces of the particles, we performed a series of control experiments with free biotin (500 μM; Sigma-Aldrich) to pre-block the biotin-binding sites on the SA, where we then spiked the solution with 5 μM pre-blocked SA. After adding 200 μM biotin-ELPs and incubating for 10 min, the particles with UV-reacted ELPs, particles with adsorbed ELPs and bare particles (representing the three experimental conditions) were separately added to this mixture. Following the same procedure, the amounts of SA sequestered by each type of particle at 25 and 40°C were estimated to test if sequestration occurred below the T_t.

The co-aggregation assay with ELPs was also conducted in porcine blood. We spiked 100 μL whole porcine blood containing sodium heparin (BioreclamationIVT, LLC) with 5 μM fluorescent SA followed by 200 μM biotin-ELP. Prior to use, the porcine blood was passed through high capacity SA chromatography cartridges (Pierce; Thermo Fisher) to remove native biotin. After 10 min of incubation, we added 20 μL of the ELP-modified particles (~10^8 particles/mL) to the mixture, and we increased the temperature above the T_t (i.e., 34°C, see Figure S2 in the Supplementary Information for more details), to 40°C, to trigger the co-aggregation of the SA/biotin-ELP complexes to the surface-bound ELP-Cys for an additional 5 min. The silicone particles with captured SA were analyzed using flow cytometry at 40°C. The molecules of SA per particle was calculated for each condition by dividing the MEFL by the average number of fluorophores on each SA molecule (provided by the manufacturer, Invitrogen), which was 4.0 in the case of the Alexa Fluor 488-labeled SA used in this study.

Acoustic separation of biomarker-particle complexes from blood cells

After triggering the co-aggregation of ELPs in blood, we diluted the mixture 100-fold with PBS warmed to 40°C to allow the acoustic radiation forces to effectively focus and separate particles and cells.[31] To form the standing wave, we actuated the lead zirconate titanate (PZT) transducer (841 WFB, 2.93 MHz resonance frequency; APC International, Ltd.) mounted on an acoustofluidic chip to 2.35 MHz using a waveform generator (33250A; Agilent Technologies, Co.) at 40.0 V peak-to-peak after amplification (25A250AM6; Amplifier Research, Co.). We then passed the solution through the acoustofluidic chip (see Figure S3 in the Supplementary Information for more details on device design[57] and flow settings through each of the inlets and outlets) at a total flow rate of 50 μL/min at 40°C using a syringe pump (Nexus 3000; Chemyx, Inc.). Solutions were collected from the "collection" and "waste" outlets. The separation efficiency was then determined by counting the number of silicone particles from the "collection" outlets and the number of blood cells from the "waste" outlet, divided by the total number of particles and cells using a hemocytometer.

To visualize the separation of particles from blood cells, Nile red dye (Sigma-Aldrich) was used to stain blood cells. This was accomplished by incubating a 20 μL Nile red solution (1 mg/mL in acetone) in 100 μL whole blood for 3 h at 4°C, followed by washing (i.e., centrifuging at 300xG for 5 min, decanting the supernatant and suspending the pellet in an equal volume of fresh PBS) to remove unabsorbed dye. The separation of silicone particles from blood cells was monitored using a fluorescence microscope (Axio Imager A2; Carl Zeiss) and imaged using a CCD camera (Axiocam) with AxioVision software.

Biomarker capture assay in porcine plasma

To assess the sensitivity of the SA capture assay, we spiked 100 μL porcine plasma containing sodium heparin (BioreclamationIVT) with different concentrations ranging from 0 to 1 μM of Alexa Fluor® 546-labeled SA (Thermo Fisher) after removing native biotin, as described earlier. Following the same procedure of capture and thermally controlled co-aggregation, the number of SA molecules per particle was determined using flow cytometry. To demonstrate the capture was biospecific, we performed a series of control experiments using plasma samples containing various amounts of SA (ranging from 0-1 μM) pre-incubated with free biotin (500 μM; Sigma-Aldrich). Finally, to compare the detection limit of our system against a commercial standard, we added biotinylated polystyrene (PS) beads (3 μm; Spherotech, C.V. in size is ~ 5%) to the porcine plasma spiked with fluorescent SA (ranging from 0-1 μM). After 15 min incubation with gentle shaking (10 min for SA capture and 5 min for co-aggregation), the amounts of sequestered SA were measured using flow cytometry. We normalized the values for molecules equivalent of SA per particle by subtracting the average value measured for the autofluorescence signal of the bare particles ($n \geq 3$). We defined the detection limit as the concentration at which the measured value was at least 3 standard deviations (3σ) above the mean of the blank group (i.e., ELP-modified particles without SA).

Thermally triggered release of biomarkers from particles

To evaluate the efficiency of the ELPs to release the captured SA with a thermal trigger, we spiked 200 μL PBS with 5 μM fluorescent SA, added 200 μM biotin-ELP and incubated for 10 min. We then added ELP-modified particles (20 μL) to the mixture and increased the temperature to 40°C for 5 min. After the co-aggregation of the SA/biotin-ELP complexes to the ELP-modified particles, the particles were stored on ice for 2 h to facilitate the release of the

SA/biotin-ELP complexes. The molecules equivalent of SA per particle was measured before and after release by flow cytometry.

Results and discussion

Functionalization of silicone particles with ELPs

GFP-ELPs containing a cysteine-rich domain (GFP-ELP-Cys) were conjugated to vinyl groups on the surfaces of particles of crosslinked polyvinylmethylsiloxane via a thiol-ene reaction facilitated by UV irradiation (see schematic depiction in Figure 2a).[50,51] Since one GFP molecule is present on each ELP, the molecules equivalent of GFP-ELP-Cys per particle can be determined by flow cytometry. We found that the silicone particles that reacted with 150 μM GFP-ELP-Cys under UV light had the highest amount of ELPs on their surface, which was significantly higher than the amounts resulting from physical adsorption ($p < 0.05$, $n = 5$; Figure 2b). After the reaction, the GFP-ELP-Cys-modified particles were visualized using confocal microscopy. We found that the silicone particles were evenly decorated with GFP-ELP-Cys, confirming the successful coating of the particles with ELPs (Figure 2c). Thus, the thiol-ene reaction was chosen to functionalize silicone particles with ELPs for the remaining experiments.

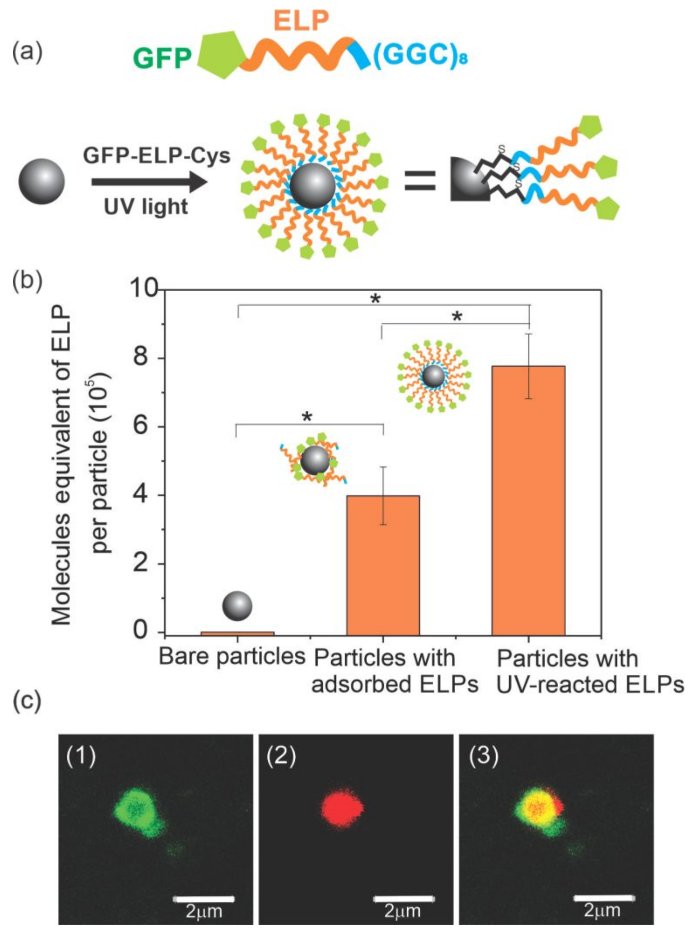

Figure 2. (a) Schematic illustration of the immobilization of GFP-ELP-Cys polypeptides (150 μM) to the surfaces of silicone particles via a thiol-ene reaction. (b) Data from flow cytometry reveals the molecules equivalent of ELP per particle for bare particles, particles with physically adsorbed ELPs and particles with UV-reacted ELPs. The asterisks indicate a significant difference between conditions ($*p < 0.05$, $n = 5$). (c) Representative confocal micrographs of a GFP-ELP-Cys-modified silicone particle: (1) green fluorescent ELP localized around the surface of a particle, (2) a Nile red-encapsulating silicone particle and (3) overlaid images from (1) and (2).

Immobilization of model biomarkers onto silicone particles via ELP co-aggregation above the T_t

Figure 3a schematically depicts the process of SA/biotin-ELP complexes being captured by microparticles with ELP-Cys immobilized on their surfaces upon heating above the T_t of the ELPs (~34°C; Figure S2). The silicone particles with UV-reacted ELP-Cys captured the highest amount of fluorescently labeled SA at 40°C, whereas the same particles captured significantly less SA at 25°C ($p < 0.05$, $n = 6$; Figure 3b). This confirms our hypothesis that biotin-ELP fusion proteins can efficiently capture SA molecules, and that SA/biotin-ELP complexes can be immobilized onto the surfaces of ELP-Cys-modified silicone particles through thermally controlled co-aggregation. Bare particles and particles with physically adsorbed ELP-Cys were used as controls. These particles captured significantly less SA compared to particles with UV-reacted ELP-Cys ($p < 0.05$). Further, no significant changes in the fluorescence intensity were observed between 25 and 40°C for the two groups ($p > 0.05$). To assess the non-specific adsorption of SA to surfaces of the particles, we pre-blocked the SA by incubating with a molar excess of biotin. Under these conditions, we found that significantly less SA was sequestered by particles with UV-reacted ELP-Cys at 40°C than for the non-blocked case ($p < 0.05$), indicating that capture of SA was largely mediated by the molecular recognition of SA by the biotin-ELP. Given these results, we used silicone particles modified with UV-reacted ELP-Cys for the remaining experiments in this study. (Subsequently herein we referred to these simply as ELP-modified particles.)

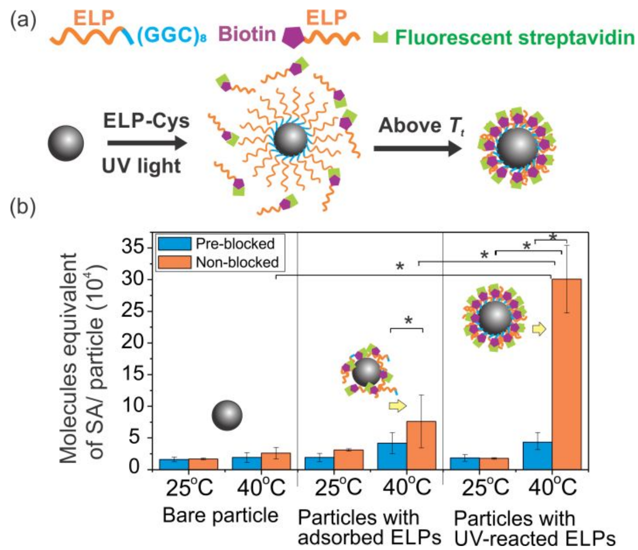

Figure 3. (a) Schematic illustration of ELP-Cys binding to silicone particles and capturing SA/biotin-ELP complexes via thermal co-aggregation. (b) The molecules equivalent of SA per particle are shown for bare particles, particles with physically adsorbed ELPs and particles with UV-reacted ELPs both below and above the T_t. Control experiments (shown in blue) were performed by pre-blocking the biotin binding sites on the SA to quantify the non-specific adsorption of SA onto the particles. The asterisks indicate a significant difference between conditions (*$p < 0.05$, $n = 6$).

Acoustic separation of biomarkers sequestered on silicone particles from diluted whole blood

After immobilizing the SA molecules on the surfaces of the silicone particles, we separated them from blood cells using an acoustofluidic device (Figure 4a and Figure S3). In this setup, the SA-sequestered particles were separated from blood cells by diluting the sample with warm buffer and flowing it through a heated acoustofluidic device supporting a resonant half-wavelength standing acoustic wave across the width of the central fluidic channel of the device. Acoustic radiation forces separated the silicone particles from cells, and laminar flow allowed the particles to exit the peripheral "collection" outlets for analysis. To establish operational parameters for the device, we performed a pilot study to separate ELP-modified silicone particles co-aggregated with SA/biotin-ELP complexes from polystyrene (PS) beads. Our device achieved a separation efficiency 97.5% in the peripheral outlets and 87.4% PS beads in the central outlet (see Figure S4 in the Supplementary Information for more details). Using the established parameters, we used the device to separate ELP-modified particles co-aggregated with SA/biotin-ELP complexes from diluted porcine blood. The fractions from the two "collection" outlets consisted of 90.3% silicone particles and 9.7% blood cells; whereas the output from the "waste" outlet consisted of 83.3% blood cells and 16.7% silicone particles in a single pass (Figure 4b). Due to the negative acoustic contrast of the silicone particles ($\varphi = -0.37 \pm 0.07$),[35] we posit the reason behind a relatively large fraction of silicone particles in the "waste" outlet was due to the high concentration of ELPs on the surfaces of the particles, reducing the magnitude of their negative acoustic contrast factor, or due to their relatively high throughput through the device, which can decrease the efficiency of separation due to scattering. The throughput was ≈5,860 cells/s or particles/s (with a sample infusion rate of 50 μL/min at a concentration of 3.52×10^5 particles/s or cells/s). Additional studies to optimize the design of particles and their throughput through the device should enhance their separation efficiency. In such studies, synthesizing particles with more negative acoustic contrast factors or of larger sizes will generate higher acoustic radiation forces, thus improving separation performance. Methods for preparing different types of negative acoustic contrast particles are described elsewhere.[35] We note that longer microchannels allow for longer residence time of particles and thus a potential for improved separation efficiencies or higher throughputs. Figure 4c,d shows micrographs of blood cells (stained with Nile red) focused along the pressure node, and silicone particles with sequestered SA (labeled with Alexa 488) focused along the pressure antinodes. We note that these images were taken from separate samples, as the Nile red dye used to visualize the blood cells was found to leach and stain the silicone particles.

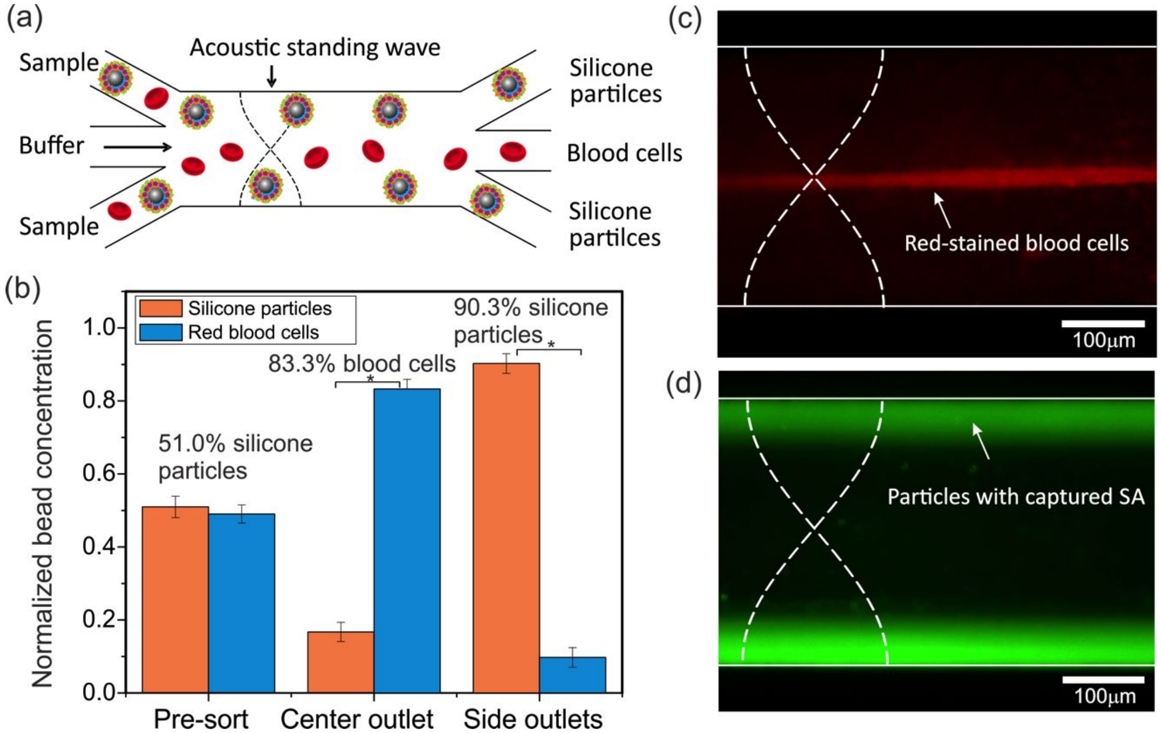

Figure 4. (a) Schematic depiction of the separation of silicone particles with captured SA from blood cells in an acoustofluidic chip. Figure is not to scale. (b) The bar graph shows the relative fraction of silicone particles and blood cells in the initial sample and collected fractions from the side outlets and center outlet after sorting. The asterisks indicate a significant difference between conditions (*$p < 0.05$, $n = 5$). (c) Stained blood cells (red) migrated to the pressure node (i.e., the center of the microchannel). (d) Silicone particles with captured SA (green) migrated to the pressure antinodes (i.e., the sides of the microchannel). The locations of the channel walls (solid lines) and the features of the acoustic standing wave (dashed lines) are denoted. Samples shown

in Figure 4c,d were introduced in the center inlet, and images were collected at the same fixed point downstream of the inlets.

To test if biomarkers remained stably associated with the particles throughout the acoustic separation process, the amount of SA per particle was assessed via flow cytometry both before and after separation. Exclusively for this test, we performed the capture assay in physiological buffer prior to mixing with blood (instead of performing the capture assay in blood) to accurately quantify the amount of SA per particle. We observed no significant difference in the amount of SA per particle before and after acoustic separation at 40°C ($p > 0.05$; see Figure S5 in the Supplementary Information for more details), suggesting that SA remained stably associated with the surfaces of the particles throughout acoustic separation.

Quantification of captured SA using flow cytometry

After acoustic separation, particles with captured biomarkers were analyzed using flow cytometry without washing. An advantage of flow cytometry is that it allows for the direct and sensitive detection of fluorescently labeled, surface-sequestered biomarkers, where non-captured fluorescent molecules generate minimal background signal.[58]

To assess the detection sensitivity of our SA capture and isolation method, we performed a capture assay in porcine plasma (~100 μL) containing different concentrations of fluorescent SA, ranging from 0 to 1 μM. After adding ELP-modified silicone particles to capture the SA via co-aggregation, the amount of SA was quantified using flow cytometry. The assay revealed a high signal-to-noise ratio, which yielded a detection limit of 0.75 nM SA in blood plasma (as defined by 3 standard deviations above the mean of the signal from the bare particle group; Figure 5a). We found that the molecules equivalent of SA per particle initially increased with increasing concentration of SA across a broad, dynamic range of 0.75 to ≈100 nM, followed by a plateau when the surfaces of the particles were likely saturated with excess SA. A biphasic curve was observed, which may be due to the fact that, at low concentrations of SA, abundant uncomplexed biotin-ELP molecules in solution were more likely to come into contact and co-aggregate with ELPs on the surfaces of particles compared to more rare and larger SA/biotin-ELP complexes; in contrast, at higher concentrations of SA, the inhibitory effect of the free biotin-ELP may be less prominent due to their decreased concentration compared to SA/biotin-ELP complexes. The possibility that one SA can bind up to four biotin/ELP molecules may also contribute to the response observed.

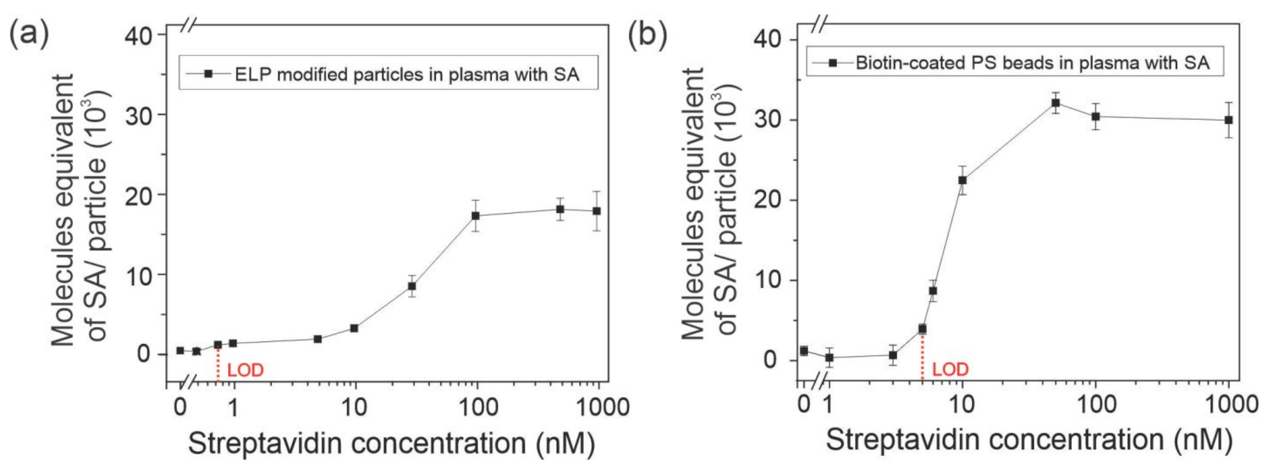

Figure 5. Molecules equivalent of SA sequestered by (a) silicone particles and (b) biotinylated PS beads (3 μm; Spherotech, Inc.) after 15 min of incubation with various amounts of SA. The values for molecules equivalent of SA per particle were normalized by subtracting the average value measured for the autofluorescence signal of the bare particles. Dashed lines indicate the limits of detection (LODs). Error bars represent the standard error of the mean ($n \geq 3$).

We compared our system to a commercial surface-binding assay, where we used the biotin-coated PS beads of the same concentration as silicone particles to detect fluorescent SA in plasma. After 15 min of incubation on a rocker at a speed of 10 rpm, the fluorescence intensity was measured using flow cytometry and a detection limit of 5 nM with a dynamic range from 5 to ≈50 nM was determined (Figure 5b). Our system demonstrated a lower detection limit (i.e., 0.75 nM, compared to 5.00 nM), which corresponds to a ≈6-fold higher sensitivity. Overall, this supports the notion that implementation of soluble ligand-peptides for protein capture enhances binding efficiency, which may lead to more sensitive detection of analytes at shorter incubation times.[59,60] We note that several assay parameters can be adjusted to further improve the detection limit, including the size, concentration and composition of the particles. For example, optimizing the size and concentration of the particles would allow each particle to capture more SA on its surface, thus increasing the fluorescence intensity per particle at low concentrations of SA, and leading to a higher detection sensitivity of the SA capture assay.

To demonstrate that the capture of SA via biotin was mediated by SA-biotin recognition, we carried out the capture assay using plasma that was pre-incubated with 20-fold molar excess of free biotin (see Figure S6 in the Supplementary Information for more details). The fluorescence from particles with non-specifically adsorbed SA was much lower than particles with specific binding, indicating that the SA capture was mediated by biotin recognition.

Release of the biomarkers from the surfaces of the particles below the T_t

After acoustic separation, the captured SA can be released from the particles by reducing the temperature of the solution below the T_t. The schematic depiction of the capture and release of SA is shown in Figure 6a. We found that more than 75% of the captured SA was released from the surfaces of the particles at a temperature (i.e., ~4°C, samples were placed on ice) lower than T_t (Figure 6b). We believe that optimizing the duration of co-aggregation, release temperature and duration of release can increase this percentage of release.

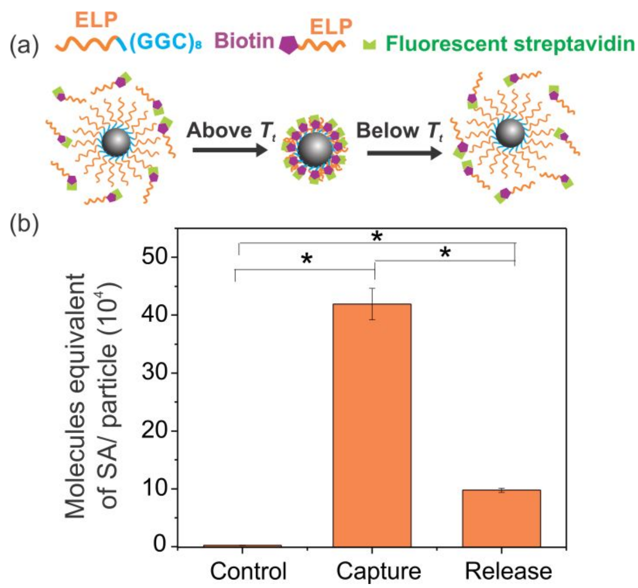

Figure 6. (a) Schematic illustration depicts the capture and release of SA from the surfaces of ELP-modified silicone particles. (b) Data from flow cytometry reveals the molecules equivalent of SA per particle for ELP-modified particles above and below the T_t (i.e., 34°C). The autofluorescence signal of bare silicone particles was measured as a control. The asterisks indicate a significant difference between conditions (*$p < 0.05$, $n = 6$).

While beyond the scope of this study, the released ELP-bound biomarkers can be enriched in buffer by exploiting the phase transition behavior of the ELPs.[61] Chen *et al.* have used ELP-Protein A fusions with specific antibodies to isolate and enrich paclitaxel.[36] Chilkoti *et al.* have demonstrated that ELPs can serve as a purification tag for target proteins that were directly fused to ELPs.[62] We also note that it is possible to dissociate biomarker/ELP complexes, or to degrade ELPs enzymatically,[63] liberating purified biomarkers as a final product of the separation process.

These purified biomarkers can be used for further analysis, including mass spectrometric analysis, immunogenetic assessment and genomic analysis (e.g., for cell-free DNA or microRNA biomarkers).

Conclusions and future outlook

We have developed an integrated system that enables the rapid capture, chip-based separation and off-chip enumeration of protein biomarkers from blood. We demonstrated that ELP-modified silicone particles can capture SA in blood within only 15 minutes of incubation. Further, we show the biomarker-particle complexes can be continuously separated from diluted whole blood in an acoustofluidic device without any washing or centrifugation steps. In addition, we achieved sorting efficiencies exceeding 90% of biomarker-particle complexes from blood cells and a 75% release efficiency of biomarkers from the particles. Importantly, we show our system is capable of nanomolar-level detections of streptavidin in blood plasma.

Other methods have been proposed for separating deformable objects, including non-inertial lift forces and pinched flow fractionation.[64–66] While these methods have achieved continuous separation of particles based on their elasticity, there are three advantages of the approach described here to separate objects by the sign of their acoustic contrast factor. First, acoustics provide control over separation by the acoustic pressure amplitude and frequency—providing additional parameters for controlling particle displacements. Second, they obviate the need for continuous flows. In acoustics, flow through the device can be stopped, and particles can be inspected while their separation is maintained by acoustic forces. Finally, acoustic standing waves exert forces on cells and elastomeric particles in opposite directions, yielding potentially higher separation efficiencies and higher throughputs.

This platform system could be extended to separate a range of biological materials, including cells, viruses and cell-free DNA, from complex biofluids by designing ELP fusion proteins that can capture said bioactive materials. For example, ELPs with antibody-binding domains derived from Protein A or Protein G were genetically designed and recombinantly synthesized to capture immunoglobulins such as IgG.[36,67,68] Further testing will be necessary to determine the capture efficiency of biomolecules with lower binding affinities. In addition, advances in microfluidic flow cytometry could allow the direct coupling of quantification means to this system,[69–72] which would further decrease the time of analysis and increase utility by providing a potentially portable and automated system for point-of-care (POC) testing.

Conflicts of interest

There are no conflicts to declare.

Acknowledgements

This work was supported by the National Science Foundation's (NSF's) Research Triangle Materials Research Science and Engineering Center (MRSEC, DMR-1121107), an NSF Graduate Research Fellowship (1106401) to K.A.O., and grants from the National Institutes of Health (R21GM111584 to G.P.L and B.B.Y.; R01GM061232 to A.C.). We thank Prof. James Lai (Univ. of Washington) for helpful technical discussions.

References

1 S. Kumar, A. Mohan and R. Guleria, *Biomarkers*, 2006, **11**, 385–405.
2 R. Mayeux, *NeuroRx*, 2004, **1**, 182–188.
3 R. Jones, *Nature*, 2010, **466**, S11–S12.
4 L. Murphy and R. W. Watson, *Nature Reviews Urology*, 2012, **9**, 464–472.
5 M. Toner and D. Irimia, *Annual Review of Biomedical Engineering*, 2005, **7**, 77–103.
6 E. Stern, A. Vacic, N. K. Rajan, J. M. Criscione, J. Park, T. M. Fahmy, M. A. Reed, B. R. Ilic, D. J. Mooney, M. A. Reed and T. M. Fahmy, *Nature Nanotechnology*, 2010, **5**, 138–142.

7 R. Etzioni, N. Urban, S. Ramsey, M. McIntosh, S. Schwartz, B. Reid, J. Radich, G. Anderson and L. Hartwell, *Nature Reviews Cancer*, 2003, **3**, 243–252.

8 S.-L. L. Liang and D. W. Chan, *Clinica Chimica Acta*, 2007, **381**, 93–97.

9 J. Comley, *Drug Discovery World*, 2012, **13**, 23–45.

10 X. Chen, Y. Ba, L. Ma, X. Cai, Y. Yin, K. Wang, J. Guo, Y. Zhang, J. Chen, X. Guo, Q. Li, X. Li, W. Wang, Y. Zhang, J. Wang, X. Jiang, Y. Xiang, C. Xu, P. Zheng, J. Zhang, R. Li, H. Zhang, X. Shang, T. Gong, G. Ning, J. Wang, K. Zen, J. Zhang and C.-Y. Zhang, *Cell Research*, 2008, **18**, 997–1006.

11 W. Kolch, C. Neusüss, M. Pelzing and H. Mischak, *Mass Spectrometry Reviews*, 2005, **24**, 959–977.

12 M. Kersaudy-Kerhoas and E. Sollier, *Lab on a Chip*, 2013, **13**, 3323–46.

13 H. N. Bhagavan and D. B. Coursin, *The American Journal of Clinical Nutrition*, 1967, **20**, 903–906.

14 C. Legido-Quigleya, C. Stella, F. Perez-Jimenez, J. Lopez-Miranda, J. Ordovas, J. Powell, F. Van-der-Ouderaa, L. Ware, J. C. Lindon, J. K. Nicholson and E. Holmes, *Biomedical Chromatography*, 2010, **24**, 737–743.

15 G. A. Theodoridis, H. G. Gika, R. Plumb and I. D. Wilson, in *Proteomic and Metabolomic Approaches to Biomarker Discovery*, Elsevier, 2013, pp. 145–161.

16 D. Fliser, S. Wittke and H. Mischak, *Electrophoresis*, 2005, **26**, 2708–2716.

17 M. Ohlin, I. Iranmanesh, A. E. Christakou and M. Wiklund, *Lab on a Chip*, 2015, **15**, 3341–3349.

18 O. Manneberg, S. Melker Hagsäter, J. Svennebring, H. M. Hertz, J. P. Kutter, H. Bruus and M. Wiklund, *Ultrasonics*, 2009, **49**, 112–119.

19 A. Lenshof and T. Laurell, *Chemical Society Reviews*, 2010, **39**, 1203.

20 P. Augustsson and T. Laurell, *Lab on a Chip*, 2012, **12**, 1742.

21 I. Iranmanesh, H. Ramachandraiah, A. Russom and M. Wiklund, *RSC Advances*, 2015, **5**, 74304–74311.

22 K. W. Cushing, M. E. Piyasena, N. J. Carroll, G. C. Maestas, B. A. López, B. S. Edwards, S. W. Graves and G. P. López, *Analytical Chemistry*, 2013, **85**, 2208–2215.

23 A. A. Tajudin, K. Petersson, A. Lenshof, A.-M. Swärd-Nilsson, L. Åberg, G. Marko-Varga, J. Malm, H. Lilja and T. Laurell, *Lab on a Chip*, 2013, **13**, 1790–1796.

24 M. Wu, Y. Ouyang, Z. Wang, R. Zhang, P.-H. Huang, C. Chen, H. Li, P. Li, D. Quinn, M. Dao, S. Suresh, Y. Sadovsky and T. J. Huang, *Proceedings of the National Academy of Sciences*, 2017, **114**, 10584–10589.

25 L. M. Johnson, L. Gao, C. W. Shields IV, M. Smith, K. Efimenko, K. Cushing, J. Genzer and G. P. López, *Journal of Nanobiotechnology*, 2013, **11**, 22–29.

26 C. W. Shields, L. M. Johnson, L. Gao and G. P. López, *Langmuir*, 2014, **30**, 3923–3927.

27 K. A. Ohiri, B. A. Evans, C. W. Shields, R. A. Gutiérrez, N. J. Carroll, B. B. Yellen and G. P. López, *ACS Applied Materials & Interfaces*, 2016, **8**, 25030–25035.

28 H. Bruus, *Lab on a Chip*, 2012, **12**, 1014.

29 M. Settnes and H. Bruus, *Physical Review E*, 2012, **85**, 016327.

30 C. Grenvall, P. Augustsson, J. R. Folkenberg and T. Laurell, *Analytical Chemistry*, 2009, **81**, 6195–6200.

31 T. Laurell, F. Petersson and A. Nilsson, *Chemical Society Reviews*, 2007, **36**, 492–506.

32 A. Lenshof, C. Magnusson and T. Laurell, *Lab on a Chip*, 2012, **12**, 1210–1223.

33 F. Petersson, A. Nilsson, C. Holm, H. Jonsson and T. Laurell, *The Analyst*, 2004, **129**, 938–943.

34 L. Gao, C. Wyatt Shields, L. M. Johnson, S. W. Graves, B. B. Yellen and G. P. López, *Biomicrofluidics*, 2015, **9**, 014105.

35 C. W. Shields, D. Sun, K. A. Johnson, K. A. Duval, A. V. Rodriguez, L. Gao, P. A. Dayton and G. P. López, *Angewandte Chemie International Edition*, 2014, **53**, 8070–8073.

36 J.-Y. Kim, S. O'Malley, A. Mulchandani and W. Chen, *Analytical Chemistry*, 2005, **77**, 2318–2322.

37 W. Hassouneh, S. R. MacEwan and A. Chilkoti, *Methods in Enzymology*, 2012, **502**, 215–237.

38 U. L. Lao, J. Kostal, A. Mulchandani and W. Chen, *Nature Protocols*, 2007, **2**, 1263–1268.

39 D. H. Kim, J. T. Smith, A. Chilkoti and W. M. Reichert, *Biomaterials*, 2007, **28**, 3369–3377.

40 L. Li, C.-K. Mo, A. Chilkoti, G. P. Lopez and N. J. Carroll, *Biointerphases*, 2016, **11**, 21009.

41 R. A. Vijayendran and D. E. Leckband, *Analytical Chemistry*, 2001, **73**, 471–480.

42 N. M. Green, *Advances in Protein Chemistry*, 1975, **29**, 85–133.

43 L. Chaiet and F. J. Wolf, *Archives of Biochemistry and Biophysics*, 1964, **106**, 1–5.

44 D. W. Urry, *Progress in Biophysics and Molecular Biology*, 1992, **57**, 23–57.

45 D. W. Urry, *The Journal of Physical Chemistry B*, 1997, **101**, 11007–11028.

46 J. Hyun, W.-K. Lee, N. Nath, A. Chilkoti and S. Zauscher, *Journal of the American Chemical Society*, 2004, **126**, 7330–7335.

47 N. Nath and A. Chilkoti, *Analytical Chemistry*, 2003, **75**, 709–715.

48 J. M. Hoffman, M. Ebara, J. J. Lai, A. S. Hoffman, A. Folch and P. S. Stayton, *Lab on a Chip*, 2010, **10**, 3130–3138.

49 A. L. Golden, C. F. Battrell, S. Pennell, A. S. Hoffman, J. J. Lai and P. S. Stayton, *Bioconjugate Chemistry*, 2010, **21**, 1820–1826.

50 T. Posner, *Berichte der Deutschen Chemischen Gesellschaft*, 1905, **38**, 646–657.

51 S. Mongkhontreerat, K. Öberg, L. Erixon, P. Löwenhielm, A. Hult and M. Malkoch, *Journal of Materials Chemistry A*, 2013, **1**, 13732–13737.

52 J. R. McDaniel, J. A. MacKay, F. G. Quiroz and A. Chilkoti, *Biomacromolecules*, 2010, **11**, 944–952.

53 A. J. Conley, J. J. Joensuu, A. M. Jevnikar, R. Menassa and J. E. Brandle, *Biotechnology and Bioengineering*, 2009, **103**, 562–573.

54 N. Brand, *Proteomics*, 2006, **6**, 6119–6120.

55 G. W. Anderson, J. E. Zimmerman and F. M. Callahan, *Journal of the American Chemical Society*, 1964, **86**, 1839–1842.

56 Spherotech Inc., *Sphero Technical Note 9(D 041106)*, 2010, 1–7.

57 C. W. Shields, D. F. Cruz, K. A. Ohiri, B. B. Yellen and G. P. López, *Journal of Visualized Experiments*, 2016, 1–7.

58 J. P. Nolan, S. Lauer, E. R. Prossnitz and L. A. Sklar, *Drug Discovery Today*, 1999, **4**, 173–180.

59 G. Hu, Y. Gao and D. Li, *Biosensors & Bioelectronics*, 2007, **22**, 1403–1409.

60 P. R. Nair and M. A. Alam, *Applied Physics Letters*, 2006, **88**, 23–26.

61 W. Hassouneh, T. Christensen and A. Chilkoti, *Current Protocols in Protein Science*, 2010, **Chapter 6**, Unit 6.11.
62 D. E. Meyer and A. Chilkoti, *Nature Biotechnology*, 1999, **17**, 1112–1115.
63 M. Shah, P. Y. Hsueh, G. Sun, H. Chang, S. M. Janib and J. A. MacKay, *Protein Science*, 2012, **21**, 743–750.
64 T. M. Geislinger and T. Franke, *Advances in Colloid and Interface Science*, 2014, **208**, 161–176.
65 C. W. Shields IV, C. D. Reyes and G. P. López, *Lab on a Chip*, 2015, **15**, 1230–1249.
66 M. Yamada, M. Nakashima and M. Seki, *Analytical Chemistry*, 2004, **76**, 5465–5471.
67 B. Madan, G. Chaudhary, S. M. Cramer and W. Chen, *Journal of Biotechnology*, 2013, **163**, 10–16.
68 R. D. Sheth, M. Jin, B. V Bhut, Z. Li, W. Chen and S. M. Cramer, *Biotechnology and Bioengineering*, 2014, **111**, 1595–1603.
69 T. D. Chung and H. C. Kim, *Electrophoresis*, 2007, **28**, 4511–4520.
70 M. E. Piyasena, P. P. Austin Suthanthiraraj, R. W. Applegate, A. M. Goumas, T. A. Woods, G. P. López and S. W. Graves, *Analytical Chemistry*, 2012, **84**, 1831–1839.
71 Y. J. Heo, D. Lee, J. Kang, K. Lee and W. K. Chung, *Scientific Reports*, 2017, **7**, 11651.
72 X. Wang, H. Gao, N. Dindic, N. Kaval and I. Papautsky, *Biomicrofluidics*, 2017, **11**, 14107.

For TOC only